Multiple Approaches to Repurposing drugs for Neuroblastoma

Laura Rank[†,*], **Ana C. Puhl**[†,*,#], **Tammy M. Havener**[‡], **Edward Anderson**[‡], **Daniel H. Foil**[†], **Kimberley M. Zorn**[†], **Natalia Monakhova**[§], **Olga Riabova**[§], **Anthony J. Hickey**[§,&], **Vadim Makarov**[§], **Sean Ekins**[†,#]

[†]Collaborations Pharmaceuticals, Inc., 840 Main Campus Drive, Lab 3510, Raleigh, North Carolina, United States of America

[‡]UNC Catalyst for Rare Diseases, Eshelman School of Pharmacy, University of North Carolina at Chapel Hill, North Carolina, United States of America

[§]Research Center of Biotechnology RAS, 119071 Moscow, Russia

[&]RTI International, Research Triangle Park, North Carolina, United States of America

Abstract

Neuroblastoma (NB) is the second leading extracranial solid tumor of early childhood with about two-thirds of cases presenting before the age of 5, and accounts for roughly 15 percent of all pediatric cancer fatalities in the United States. Treatments against NB are lacking, resulting in a low survival rate in high-risk patients. A repurposing approach using already approved or clinical stage compounds can be used for diseases for which the patient population is small, and the commercial market limited. We have used Bayesian machine learning, *in vitro* cell assays, and combination analysis to identify molecules with potential use for NB. We demonstrated pyronaridine (SH-SY5Y IC_{50} 1.70 μM, SK-N-AS IC_{50} 3.45 μM), BAY 11-7082 (SH-SY5Y IC_{50} 0.85 μM, SK-N-AS IC_{50} 1.23 μM), niclosamide (SH-SY5Y IC_{50} 0.87 μM, SK-N-AS IC_{50} 2.33 μM) and fingolimod (SH-SY5Y IC_{50} 4.71 μM, SK-N-AS IC_{50} 6.11 μM) showed cytotoxicity against NB. As several of the molecules are approved drugs in the US or elsewhere, they may be repurposed more readily for NB treatment. Pyronaridine was also tested in combinations in SH-SY5Y cells and demonstrated an antagonistic effect with either etoposide or crizotinib. Whereas when crizotinib and etoposide were combined with each other they had a synergistic effect in these cells. We have also described several analogs of pyronaridine to explore the structure-activity relationship against cell lines. We describe multiple molecules demonstrating cytotoxicity against NB and the further evaluation of these molecules and combinations using other NB cells lines and *in vivo* models will be important in the future to assess translational potential.

Keywords

Drug Discovery; Machine learning; Neuroblastoma; Pyronaridine; Repurposing

BACKGROUND

Neuroblastoma (NB) is a rare cancer of nerve tissue that can arise anywhere in the sympathetic nervous system derived from the embryonic neural crest. NB accounts for 12%–15% of all childhood cancer-related deaths and is the most common and deadly extracranial tumor [1, 2] with a median age at diagnosis of 18 months [1, 3]. Two-thirds of the NB cases present before the age of 5 and 40 percent of patients are diagnosed before one year of age while the number steadily decreases with increasing age [3]. NB develops from immature nerve cells, referred to as neuroblasts. When the neuroblast itself does not mature, a cancer-causing malformation occurs as early as *in utero* [4]. NB is most common in the adrenal glands however, this cancer can be found in other areas of the body (linked to embryonic development from the neuroblast), including the chest, spinal cord, and abdomen. NB therefore remains a therapeutic challenge and approximately 800 patients are diagnosed each year in the United States [5]. NB is also characterized by a condition known as opsoclonus-myoclonus ataxia syndrome [6]. This syndrome consists of three main symptoms: opsoclonus (conjugate, multidirectional, chaotic eye movements), myoclonus (limb jerking that can also involve the head and face) and truncal ataxia, which can cause gait imbalance, sleep disturbance, cognitive dysfunction, and behavioral changes [3]. Unfortunately, NB mimics the symptoms of several other diseases, and diagnosis often occurs after the cancer has already disseminated throughout the body. Additionally, the prognosis worsens with increased age and advanced stage cancer [7].

Suggested cellular targets to treat NB include the Cannabinoid Receptor 2 (CNR2), Mitogen-Activated Protein Kinase 8 (MAPK8) [8] and Tyrosine kinase ALK/TRK. Multiple inhibitors of ALK/TRK have subsequently been identified for treatment, such as crizotinib, ceritinib, alectinib, lorlatinib and entrectinib [9]. An approach to identify new drugs for diseases that is attracting increasing attention is to use those that are already approved or at the clinical stage and repurpose them. This can be achieved using computational models for the disease or target to virtually screen clinically approved compounds and then test predicted compounds *in vitro* [10]. An alternative approach is to take a commercial library of FDA-approved drugs or clinical-stage drugs and test them all *in vitro* [11]. There have been several *in vitro* drug repurposing studies that have identified FDA-approved drugs that inhibit NB. For example, using a high-content imaging approach, over 300 drugs were tested on 3D spheroids of NB cells *in vitro* [12]. Two multiple tyrosine kinase inhibitors, ponatinib and axitinib, were proposed as promising candidates from this study as both drugs showed induction of cell-cycle block, apoptosis, and inhibition of colony formation [12]. Ponatinib consistently affected migration and inhibited invasion of NB cells as well as inhibited tumor growth in orthotopic NB mice [12]. The MYC family of transcription factors is a major driver of human cancer and is a potential therapeutic target for NB as MYCN is frequently activated in NB cells [3]. An important pathway regulated by MYC is the CKS1/SKP2/

p27^{Kip1} axis, and the antidepressant drug fluoxetine disrupts CKS1/SKP2/p27^{Kip1} signaling [13].

Overall, few computational repurposing approaches have been applied to NB. For example, a pathway approach called iPANDA was used to identify the non-FDA approved antimicrobial taurolidine. Taurolidine affects MAPK and IL-10 signaling pathways which are cytotoxic to NB *in vitro* while *in vivo* xenograft models showed decreased tumor growth and increased survival [14]. Combining computational, 2D and 3D cell-based approaches [15] as well as patient-derived xenografts [16] may also represent another pathway to identifying new drugs for NB. Recently, analysis of whole-genome, whole-exome and/or transcriptome data from 702 neuroblastoma samples illustrated that forty percent of samples harbor at least one recurrent driver gene alteration, and most aberrations, including MYCN, ATRX, and TERT alterations, differ in frequency by age [17]. COSMIC mutational signature 18, is the most common cause of driver point mutations in NB, including most Anaplastic Lymphoma Kinase (ALK) and Ras-activating variants [17]. Currently, the frontline chemotherapeutic drugs (e.g., etoposide, doxorubicin, and cisplatin) for treating NB are all DNA damaging agents [18]. Several clinical trials for NB have involved ALK inhibitors, but patients with mutations in this protein will likely not respond to treatment and new therapies are therefore still needed. ALK is a receptor tyrosine kinase that falls within the insulin receptor superfamily. ALK expression is often restricted to developing nervous system tissues and expression levels are much lower in mature, adult brains [19]. Mutation and amplification of the ALK gene is associated with both familial (~1/2 familial cases) and somatic (9% primary NB tumors and 14% high risk) NB cases [19]. Single base mutations in regulatory regions of the kinase domain of ALK promote ligand independent signaling of ALK [19]. The three most common single base pair mutations (R1275, F1174, and F1245) represent ~85% of NB ALK mutations [19]. ALK is therefore an ideal target for anti-cancer therapeutics and several tyrosine kinase inhibitors (TKIs) (entrectinib and crizotinib) have shown promise in preclinical studies against NB [20]. However, clinical studies have also shown that TKIs have differential effects on NB cell lines with different ALK mutations [20].

In the absence of other options for potential treatments besides chemotherapy, it is important that additional small molecules are identified for NB. We, therefore, used a combination of machine learning techniques and *in vitro* cell-based assays with the NB cell lines SH-SY5Y[21], SK-N-AS[22], and fibrosarcoma HT-1080 cell lines for comparison for drug discovery of molecules for NB. We have now identified multiple clinical-stage, approved drugs, and novel molecules with promising *in vitro* activity against NB that may represent useful starting points for future lead optimization and *in vivo* testing.

RESULTS

Machine learning model and *in vitro* testing

We built a Bayesian machine learning model using SH-SY5Y inhibition data that is publicly available on CHEMBL which resulted in a five-fold receiver operator characteristic (ROC) value of 0.94 at a threshold of 1.68 μM (Figure 1). All model statistics were >0.73 suggesting it would be a useful model for external validation. We, therefore, used this model

to score an in-house library of 260 compounds and prioritize compounds for testing (Table S1). From these, we identified fingolimod that was active (IC_{50} of 4.71 μM, Figure 2, Table 1). This compound was also tested in SK-N-AS cells and showed an IC_{50} 6.11 μM (Figure 2, Table 1).

Cell assays

We also performed cell-based screening of compounds (nilotinib, chlorpropamide, GW2961115, lumefantrine, mirtazapine, arbidol, dipyridamole, mefexamide hydrochloride, nimorazole, quinacrine, pyronaridine, BAY 11-7082, niclosamide and pyronaridine) and identified BAY 11-7082 (IC_{50} 0.85 μM), niclosamide (IC_{50} 0.87 μM) and pyronaridine (IC_{50} 1.70 μM) as active against the SH-SY5Y cell line (Figure 2, Table 1). These molecules were also scored with our SH-SY5Y inhibition machine learning model for comparison (Table S1). These compounds were further tested in SK-N-AS cells and had similar levels of inhibition: pyronaridine IC_{50} 3.45 μM, BAY 11-7082 IC_{50} 1.23 μM and niclosamide IC_{50} 2.33 μM (Figure 2, Table 1).

We explored the structure-activity relationship and synthesized analogs of pyronaridine, which were then evaluated in the SH-SY5Y and SK-N-AS NB cell lines as well as in HT1080 fibrosarcoma cell lines. The pyronaridine analogs 12126038 and 12126040 showed potency comparable to pyronaridine, with IC_{50}'s of 3.41 μM and 1.20 μM, respectively in SH-SY5Y (Figure 2B), and in SK-N-AS with IC_{50}'s of 5.40 μM and 3.89 μM (Figure 2D). 12126038 and 12126040 also showed IC_{50}'s of 6.09 μM and 3.6 μM respectively for fibrosarcoma HT1080 cells (Figure 2E). The structures of these and other pyronaridine analogs and IC_{50} values in different cell lines are described in Table 1.

Combination Analysis

BRAID analysis [23] (Figure S1) of pyronaridine with crizotinib as well as pyronaridine with etoposide *in vitro* inhibition data from the checkerboard assay indicates an antagonistic effect of these molecules in SH-SY5Y neuroblastoma cells as both have negative κ values. Interestingly, a synergistic affect was identified using BRAID analysis with the combination of crizotinib and etoposide with a κ of 3.46 (Table 2).

Cathepsin D

We evaluated if pyronaridine could inhibit Cathepsin D using a fluorescent enzymatic assay and found pyronaridine inhibited Cathepsin > 50% at the highest concentration tested (200 μM, Figure S2). This might however be physiologically relevant because pyronaridine is a lysosomotropic compound accumulating in the lysosome [24].

DISCUSSION

The efficacy of ALK inhibitors in patients with ALK-mutant neuroblastoma is limited, and there is therefore a need to improve their effectiveness in these patients. ALK F1174L and F1174C mutations were previously identified as acquired resistance mutations in oncogenic ALK fusion proteins during crizotinib and ceritinib treatments, respectively [25, 26]. In the clinical studies of crizotinib and ceritinib in pediatric patients with ALK-

driven neuroblastoma, most tumors harboring R1275Q-mutated ALK did not respond to the treatments even though cells with the R1275Q mutation are sensitive to both drugs [27]. This suggests there is still a need for discovery of new molecules for NB. We used SH-SY5Y and SK-N-AS NB cell lines for our drug discovery studies. SH-SY5Y has non-amplified MYCN, it has the ALK F1174 L mutation, and it is TP53 WT [28], while SK-N-AS has a single copy of the MYCN gene (thus showing no overexpression of this gene [29]), the cells express WT ALK at low levels [30] and a truncated p53 (β isoform) [31]. Therefore, in SK-N-AS, the p53β isoform is unable to induce endogenous p21 expression [31]. A previous study has shown that in NB SH-SY5Y cells bearing the wild-type p53, the p53 accumulated in response to cisplatin and can promote apoptosis, whereas SK-N-AS cells, which have a truncated form of p53 did not undergo apoptosis [32].

Our SH-SY5Y inhibition Bayesian model generated with publicly available data had excellent 5-fold cross validation statistics (Figure 1) and fingolimod (Figure 2) was identified using this. We have also described a cell-based screening for NB which resulted in the identification of several new hits with promising activity *in vitro*. In our study, fingolimod showed an IC_{50} 4.71 μM in SH-SY5Y and an IC_{50} 6.11 μM in SK-N-AS (Figure 2, Table 1) and represents an off-patent FDA approved drug that targets sphingosine-1-phosphate as a receptor modulator for lymphocyte circulation and in turn, acts as an immunomodulator. Fingolimod is currently used to treat multiple sclerosis [33]. Interestingly, this molecule has previously been identified as active against NB [34] and the sphingosine-1-phosphate receptor is considered an important target for chemoresistance [35]. We also identified BAY-7082, an NF-κB inhibitor, that is also known to induce apoptosis and S-phase arrest in gastric cancer cells [36]. BAY 11-7082 is an anti-inflammatory agent due to its ability to prevent NF-KB activation [37, 38] by inhibiting protein tyrosine phosphorylation and thereby blocking the function of IKK, effectively maintaining NFKB in an in-active form [37]. Inflammation is associated with cancer phenotypes as it promotes DNA damage, angiogenesis, and cell proliferation (activated NF-KB prevents apoptosis) [39]. BAY 11-7082 showed an improved IC_{50} in NB cells over crizotinib and entrectinib, demonstrating an IC_{50} of 0.85 μM in SH-SY5Y and IC_{50} 1.35 μM in SK-N-AS NB cell lines (Figure 2 A, C). BAY 11-7082 (30 μM) induced complete cell death in all 10 multiple myeloma cell lines as well as in the large majority of primary multiple myeloma samples [40]. BAY 11-7082 has previously shown anti-tumor effects on bladder, breast, esophageal, lung, and gastric cancers [41-44]. However, BAY 11-7082 has not previously been in clinical trials against any cancers to our knowledge. The antiparasitic niclosamide was also identified in this study (IC_{50} 0.87 μM in SH-SY5Y and IC_{50} 2.33 μM in SK-N-AS cells, Figure 2A, C) and is a drug used for treating tapeworm, which is part of World Health Organization's List of Essential Medicines. This drug has been shown to have several other uses [45, 46] although it is poorly orally available. Niclosamide was recently identified for NB using a gene expression-based approach and demonstrated efficacy in a xenograft model [47] SK-N-DZ (MYCN-amplified) and SK-N-AS (MYCN-nonamplified). Notably, treatment of these xenografts with niclosamide led to reduced tumor growth and improved survival with no apparent toxicity [47].

A compound of interest, based on our previous work [48], is the antimalarial pyronaridine, which we have now shown has an IC_{50} of 1.7 μM in SH-SY5Y (Figure 2A) and IC_{50}

of 3.45 μM in the SK-N-AS cell lines. We have previously demonstrated cytotoxicity for this molecule against Vero (IC$_{50}$ 1.3 μM [49]) HeLa (IC$_{50}$ 3.1-4.1 μM [50]) and most recently tested in A549+ACE2 and other human cell lines (IC$_{50}$ >10 μM [48]) cells. Artesunate-pyronaridine (Pyramax) is a combination therapy for malaria [51], that has been approved in Europe since 2017. Pyronaridine is an approved drug for malaria despite having a Mannich base group which has been associated with promiscuous compounds. Our group has been testing the activity of this compound extensively among many targets, and we have found that it does not appear to be promiscuous. For example, screening of pyronaridine (tested at 1 μM) against 485 kinases identified only two as having mean percent inhibition greater than 30% including CAMK1 (35%) and MELK (31%) [52]. Pyronaridine has a well-characterized antiviral activity against select viruses e.g. Ebola and COVID-19 *in vitro* [48, 53] and *in vivo* [49, 52] but does not appear to target many other viruses as described in these publications. Pyronaridine has previously been shown to have potent cytotoxicity on human breast and hematological cancer cells through induction of apoptosis [54]. Pyronaridine has been screened by the National Cancer Institute developmental therapeutics program against various breast, central nervous system, colon, leukemia, melanoma, non-small cell lung cancer, ovarian, prostate and renal cancer cell lines [55] but not neuroblastoma. A study of pyronaridine as a single oral dose (400 mg) given to a healthy volunteer found a C$_{max}$ in plasma of 495.8 ng/ml at a T$_{max}$ of 0.5 h [51, 56], which provides a concentration close to 1 μM, however, pyronaridine preferentially associates with blood cells and is highly plasma protein bound [51], which suggests that it can potentially reach the concentration necessary to have an effect on NB cells at a higher dose. Pyronaridine induced apoptosis *via* mitochondrial depolarization, Caspase 3 activation, inhibition of cell cycle progression and by directly intercalating with cellular DNA at high concentrations [54]. The pro-apoptotic activity of pyronaridine and its capacity to inhibit cancer cell growth have led to the potential use for the treatment of cancer. In addition, we have found inhibition of Cathepsin D at high concentrations (Figure S2). This target is unlikely to have a role in the cytotoxicity observed in NB, since pyronaridine is a lysosomotropic drug [24]. Cathepsin is well known aspartyl protease and is an important regulator of apoptotic pathways in cells [57]. A study performed on the human SH-SY5Y cell line demonstrated the cathepsin D involvement in the mitophagy process [58]. High levels of cathepsin D were also observed in breast, ovarian, colorectal, prostate, bladder cancer and melanoma [57]. Cathepsin D was additionally shown to have pro-angiogenesis, pro-apoptotic, pro-invasive and pro-metastatic properties [57]. In recent research, it has become evident that the lysosome is important in drug resistance phenotypes [59]. As pyronaridine is a lysosomotropic compound [24], we evaluated combination therapies of pyronaridine with etoposide and pyronaridine with crizotinib, to verify if they had any synergistic effect. Because of the weak base characteristics of lysosomotropic compounds, they can accumulate in the lysosomal lumen and elevate pH, inducing lysosomal membrane permeabilization [60]. One possibility for combination therapies to overcome resistance is to explore the use of lysosomotropic adjuvants, that could cause intracellular redistribution of chemotherapic drugs from the lysosomal lumen to the cytosol and subsequently to their sites of action [59]. Interestingly, pyronaridine did not enhance the effect of etoposide, showing a κ −0.746 in the BRAID analysis, showing a mild antagonistic effect if these drugs are used in combination (Table 2 and Fig S1B). Etoposide is a widely used chemotherapy

medication for the treatment of several types of cancer including testicular cancer, lung cancer, lymphoma, leukemia, neuroblastoma, and ovarian cancer. Etoposide forms a ternary complex with DNA and the topoisomerase II (Topo II) enzyme. Our combination treatment *in vitro* showed that etoposide and crizotinib work synergistically (Table 2, Fig S1C) as determined by BRAID analysis with a κ of 3.46. This was expected, since crizotinib and another topoisomerase inhibitor, topotecan, are reported to also act synergistically [61, 62]. Cancer cells rely on Topo II more than healthy cells since they divide more rapidly. Therefore, this causes errors in DNA synthesis and promotes apoptosis of the cancer cell [63]. Interestingly, pyronaridine has been suggested to function as an inhibitor of Topo II in *P. falciparum in vitro*, with a concentration of 11 μM required for complete inhibition of DNA decatenation by the parasite enzyme [64]. Subsequently, it was found that pyronaridine showed little inhibitory activity against *P. falciparum* Topo II *in situ*, with the parasite maintained under continuous culture *in vitro* and it was concluded that *P. falciparum* Topo II is not the specific target of pyronaridine in this parasite [64]. To our knowledge, the activity of pyronaridine against human Topo II has not been investigated. Pyronaridine and crizotinib showed a mild antagonist effect, with a κ −0.640 (Table 2, Figure S1A).

Treatment of NB patients diverges extensively between the different risk groups [1] as treatment of high-risk patients involves an intense induction chemotherapy regimen that includes cisplatin, vincristine, carboplatin, etoposide and cyclophosphamide [1]. NB is therefore one of the deadliest malignancies of childhood and needs refinement of the current treatment protocols, including the use of more targeted therapies, (both pharmacologically and cellular) which more closely reflects the molecular landscape of individual tumors. This will require the continued analysis of the influence of cells within the tumor microenvironment in order to search for novel therapy options [1]. We used a combination of machine learning techniques and cell-based assays to identify molecules with potential use for NB treatment. We identified several molecules, with low μM NB activity for this cancer including niclosamide, BAY-7082, pyronaridine and pyronaridine analogs (12126038 and 12126040) in the SH-SY5Y NB cell line.

The relapse and chemoresistance in cancers, including NB, is often associated with the inactivation of the p53 tumor suppressor. p53 mutations are unusual in human NB but, when they do occur, are found in post-chemotherapy tumors. We studied the compounds identified for SH-SY5Y in SK-N-AS NB cells. SK-N-AS presents C-terminal homozygous deletion in p53 [32]. Pyronaridine and analogs 12126038 and 12126040 were also tested in SK-N-AS cells, with similar IC_{50}s (Table 1, Fig 2 D) suggesting no impact for p53. Interestingly, pyronaridine, pyronaridine analogs, niclosamide and BAY-7082 showed increased potency when compared to crizotinib in the SK-N-AS NB cell lines (Table 1). Some of these compounds could perhaps be used as a starting point to develop higher affinity inhibitors for NB and further understand their mechanism. Besides NB SH-SY5Y and SK-N-AS cells, these compounds were also active against fibrosarcoma HT-1080 cells which might suggest a use in further cancers (Table 1). Pyronaridine provides a relatively new scaffold to be explored for cancer treatments as the major developments in this field over the past decades have been focused on developing kinase inhibitors. Since it has been shown that pyronaridine is safe to use in humans suffering from malaria from the various clinical trials [51], it could also have potential use as a therapeutic against cancer. The combination of

artesunate-pyronaridine is on the WHO list of medicines for malaria. A single-oral dose (400 mg) of pyronaridine given to a healthy volunteer showed a Cmax in plasma of 495.8 ng/mL at a Tmax of 0.5 h, which gives a concentration close to 1 μM [51, 56]. In our study, pyronaridine showed an IC_{50} 1.70 μM in SH-SY5Y which is very close to a Cmax of 1 μM. We also describe BAY 11-7082 as having an improved IC_{50} against NB than crizotinib and entrectinib in NB SH-SY5Y and SK-N-AS cells, and this compound might also be worthy of further evaluation in other NB cells lines that are refractory to treatment with ALK inhibitors.

In conclusion, this work builds on our earlier efforts demonstrating the application of Bayesian machine learning models for chordoma and their application to scoring compounds prior to *in vitro* testing [65]. We have demonstrated how both computational and focused *in vitro* screening offer compound selection and repurposing opportunities for testing against other cancers *in vitro*.

METHODS

Compounds

Compounds fingolimod, BAY 11-7082, niclosamide, entrectinib and crizotinib were purchased from MedChemExpress (MCE, Monmouth Junction, NJ). Pyronaridine tetraphosphate was purchased from BOC Sciences (Shirley, NY). Etoposide was purchased from Chemspace (Monmouth Junction, NJ). Quinacrine hydrochloride was purchased from Cayman Chemical (Ann Arbor, MI). Compounds were dissolved in DMSO before dilution in cell culture media for cell-based assays. Pyronaridine analogs were synthesized as previously reported [66].

Machine learning

Public data from ChEMBL [67] was obtained for compounds screened against the SH-SY5Y cell line (IC_{50} data from Target ID 614910) and then used to generate a Bayesian machine learning model with Assay Central software [68] and the extended connectivity fingerprint (ECFP6) descriptor. Assay Central models include the following metrics for internal predictive performance by five-fold cross-validation: Recall, Precision, Specificity, F1-Score, Receiver Operating Characteristic (ROC) curve, Cohen's Kappa, and the Matthews Correlation Coefficient. Classification models require an activity threshold, and we have applied a threshold selection to optimize performance. This model was then used to score an in-house library (totaling 260 compounds at the time) before the selection of several compounds for testing. Assay Central predictions include a probability-like score (were values above 0.5 considered an active prediction) and an applicability score which assesses the representation of the predicted molecule within the training set [69].

Cell lines and culture

SH-SY5Y NB cells were generously provided by the Catalyst for Rare Diseases (UNC Eshelman School of Pharmacy). SK-N-AS NB and CCD-sk fibroblast cells were purchased from the Tissue Culture Facility at the University of North Carolina at Chapel Hill. HT1080 fibrosarcoma cells were purchased from Sigma Aldrich. All cell lines were cultured with

a 1:1 mixture of DMEM and Ham's F12 Medium with L-glutamine and 15 mM HEPES (Gibco, Life Technologies, NY, USA) supplemented with 10% Fetal Bovine Serum (FBS) (Invitrogen). All cells were cultured in an atmosphere of 37°C and 5% CO_2.

Cell viability assay and IC_{50} determination

NB (SH-SY5Y and SK-N-AS) and fibrosarcoma (HT1080) cells were seeded into clear, flat bottom 96-well plates at a density of $1x10^4$ cells/well in a total volume of 200 μl culture media containing drugs dissolved in DMSO starting 50 μM and subsequently diluted two-fold for an additional 8 dilutions (final 0.195 μM) or DMSO alone. DMSO was present in all wells at a final concentration of 0.5%. Cells containing drug or DMSO alone were incubated for 48 h at 37°C, 5% CO_2 after which resazurin (Sigma Aldrich) was added to a final concentration of 0.0125 mg/ml to measure cell viability. Fluorescence was measured after incubating the cells with resazurin for 8 h for NB cells and for 3 h for fibrosarcoma cells by Spectramax ID5 (Molecular Devices). Fluorescence intensity was measured using an excitation filter of 544 nm and an emission filter of 590 nm. Each experiment contained 3 replicates of each drug concentration and all experiments were performed at least twice. Percent inhibition of each drug was calculated relative to the DMSO-only control. Non-linear regression analysis was performed using Prism version (Version 8.4.1, GraphPad Software, San Diego, CA) was used to determine the 50% inhibitory concentration (IC_{50}) from fitted curves (four parameter log agonist versus response variable slope). Error bars of dose-response curves represent the SEM of replicates.

Dual compound synergy assays and BRAID analysis

NB SH-SY5Y cells were seeded into 96-well plates at a density of $1x10^4$ cells/well in a total volume of 200 μl culture media containing either a single drug dissolved in DMSO, two drugs (combination) both of which were dissolved in DMSO, or DMSO alone (0.5%). Drug combinations were set up in a 6 x 6 matrix with 1:3 dilutions of drug starting at 25 μM. Cells were incubated in the presence of a single drug, drugs in combination, or DMSO alone for 48 h 37°C, 5% CO_2, after which resazurin (Sigma Aldrich) was added to a final concentration of 0.0125 mg/ml to measure cell viability. Fluorescence was measured after incubating the cells with resazurin for 8 h using an Spectramax ID5 (Molecular Devices) and an excitation filter of 544 nm and an emission filter of 590 nm. Each experiment was repeated in quadruplicate. Determination of synergy was analyzed for synergistic, additive, or antagonistic effects of the drugs in combination using or BRAID software [23] where k represents a quantitative synergy value, k < 0 implies antagonism, k = 0 implies additivity, and k > 0 implies synergy [23].

Cathepsin D

We tested the activity of pyronaridine against Cathepsin D using the Abcam (Cambridge, UK) Cathepsin Inhibitor Screening Kit, which is a fluorescence-based assay that utilizes the preferred cathepsin D substrate sequence GKPILFFRLK(Dnp)-D-R-NH2) labeled with MCA according to manufacturer's instructions with a few modifications. The assay was performed using 384 well plates in a total volume of 25 μL reaction. Dose-response curves were performed at 37 °C for 2 h, and pyronaridine was pre-incubated with Cathepsin D for 15 min prior to adding the substrate. Cathepsin D cleaves the synthetic substrate to release

the quenched fluorescent group MCA, which might then easily be measured employing a fluorometer or fluorescence plate reader at Ex/Em = 320/420 nm. The relative efficacy of test inhibitors is compared to the positive control inhibitor, Pepstatin A ($IC_{50} < 0.1$ nM).

Supplementary Material

Refer to Web version on PubMed Central for supplementary material.

ACKNOWLEDGMENTS

DATA AND SOFTWARE AVAILABILITY

Public data from ChEMBL [67] was obtained for compounds screened against the SH-SY5Y cell line (IC_{50} data from Target ID 614910) and then used to generate a Bayesian machine learning model with our proprietary software Assay Central[68].

ABBREVIATIONS USED

CNR2	Cannabinoid Receptor 2
MAPK8	Mitogen-Activated Protein Kinase 8
NB	Neuroblastoma
TKIs	tyrosine kinase inhibitors

REFERENCES

[1]. Johnsen JI, Dyberg C, Wickström M, Neuroblastoma-A Neural Crest Derived Embryonal Malignancy, Front Mol Neurosci, 12 (2019) 9. [PubMed: 30760980]

[2]. Moreno L, Barone G, DuBois SG, Molenaar J, Fischer M, Schulte J, Eggert A, Schleiermacher G, Speleman F, Chesler L, Geoerger B, Hogarty MD, Irwin MS, Bird N, Blanchard GB, Buckland S, Caron H, Davis S, De Wilde B, Deubzer HE, Dolman E, Eilers M, George RE, George S, Jaroslav S, Maris JM, Marshall L, Merchant M, Mortimer P, Owens C, Philpott A, Poon E, Shay JW, Tonelli R, Valteau-Couanet D, Vassal G, Park JR, Pearson ADJ, Accelerating drug development for neuroblastoma: Summary of the Second Neuroblastoma Drug Development Strategy forum from Innovative Therapies for Children with Cancer and International Society of Paediatric Oncology Europe Neuroblastoma, Eur J Cancer, 136 (2020) 52–68. [PubMed: 32653773]

[3]. Matthay KK, Maris JM, Schleiermacher G, Nakagawara A, Mackall CL, Diller L, Weiss WA, Neuroblastoma, Nat Rev Dis Primers, 2 (2016) 16078. [PubMed: 27830764]

[4]. Voute PA Jr., Wadman SK, van Putten WJ, Congenital neuroblastoma. Symptoms in the mother during pregnancy, Clin Pediatr (Phila), 9 (1970) 206–207. [PubMed: 5445738]

[5]. Izbicki T, Mazur J, Izbicka E, Epidemiology and etiology of neuroblastoma: an overview, Anticancer Res, 23 (2003) 755–760. [PubMed: 12680179]

[6]. Meena JP, Seth R, Chakrabarty B, Gulati S, Agrawala S, Naranje P, Neuroblastoma presenting as opsoclonus-myoclonus: A series of six cases and review of literature, J Pediatr Neurosci, 11 (2016) 373–377. [PubMed: 28217170]

[7]. Stiller CA, Bunch KJ, Trends in survival for childhood cancer in Britain diagnosed 1971-85, Br J Cancer, 62 (1990) 806–815. [PubMed: 2173943]

[8]. Almstedt E, Elgendy R, Hekmati N, Rosen E, Warn C, Olsen TK, Dyberg C, Doroszko M, Larsson I, Sundstrom A, Arsenian Henriksson M, Pahlman S, Bexell D, Vanlandewijck M, Kogner P, Jornsten R, Krona C, Nelander S, Integrative discovery of treatments for high-risk neuroblastoma, Nat Commun, 11 (2020) 71. [PubMed: 31900415]

[9]. Pacenta HL, Macy ME, Entrectinib and other ALK/TRK inhibitors for the treatment of neuroblastoma, Drug Des Devel Ther, 12 (2018) 3549–3561.

[10]. Urbina F, Puhl AC, Ekins S, Recent advances in drug repurposing using machine learning, Curr Opin Chem Biol, 65 (2021) 74–84. [PubMed: 34274565]

[11]. Vignaux PA, Minerali E, Lane TR, Foil DH, Madrid PB, Puhl AC, Ekins S, The Antiviral Drug Tilorone Is a Potent and Selective Inhibitor of Acetylcholinesterase, Chem Res Toxicol, 34 (2021) 1296–1307. [PubMed: 33400519]

[12]. Sidarovich V, De Mariano M, Aveic S, Pancher M, Adami V, Gatto P, Pizzini S, Pasini L, Croce M, Parodi F, Cimmino F, Avitabile M, Emionite L, Cilli M, Ferrini S, Pagano A, Capasso M, Quattrone A, Tonini GP, Longo L, A High-Content Screening of Anticancer Compounds Suggests the Multiple Tyrosine Kinase Inhibitor Ponatinib for Repurposing in Neuroblastoma Therapy, Mol Cancer Ther, 17 (2018) 1405–1415. [PubMed: 29695637]

[13]. Bibbo S, Lamolinara A, Capone E, Purgato S, Tsakaneli A, Panella V, Sallese M, Rossi C, Ciufici P, Nieddu V, De Laurenzi V, Iezzi M, Perini G, Sala G, Sala A, Repurposing a psychoactive drug for children with cancer: p27(Kip1)-dependent inhibition of metastatic neuroblastomas by Prozac, Oncogenesis, 9 (2020) 3. [PubMed: 31900399]

[14]. Swift L, Zhang C, Kovalchuk O, Boklan J, Trippett T, Narendran A, Dual functionality of the antimicrobial agent taurolidine which demonstrates effective anti-tumor properties in pediatric neuroblastoma, Invest New Drugs, (2019).

[15]. Nolan JC, Frawley T, Tighe J, Soh H, Curtin C, Piskareva O, Preclinical models for neuroblastoma: Advances and challenges, Cancer Lett, 474 (2020) 53–62. [PubMed: 31962141]

[16]. Kamili A, Gifford AJ, Li N, Mayoh C, Chow SO, Failes TW, Eden GL, Cadiz R, Xie J, Lukeis RE, Norris MD, Haber M, McCowage GB, Arndt GM, Trahair TN, Fletcher JI, Accelerating development of high-risk neuroblastoma patient-derived xenograft models for preclinical testing and personalised therapy, Br J Cancer, 122 (2020) 680–691. [PubMed: 31919402]

[17]. Brady SW, Liu Y, Ma X, Gout AM, Hagiwara K, Zhou X, Wang J, Macias M, Chen X, Easton J, Mulder HL, Rusch M, Wang L, Nakitandwe J, Lei S, Davis EM, Naranjo A, Cheng C, Maris JM, Downing JR, Cheung NV, Hogarty MD, Dyer MA, Zhang J, Pan-neuroblastoma analysis reveals age- and signature-associated driver alterations, Nat Commun, 11 (2020) 5183. [PubMed: 33056981]

[18]. Hara J, Development of treatment strategies for advanced neuroblastoma, Int J Clin Oncol, 17 (2012) 196–203. [PubMed: 22588779]

[19]. Trigg RM, Turner SD, ALK in Neuroblastoma: Biological and Therapeutic Implications, Cancers (Basel), 10 (2018).

[20]. Umapathy G, Mendoza-Garcia P, Hallberg B, Palmer RH, Targeting anaplastic lymphoma kinase in neuroblastoma, APMIS, 127 (2019) 288–302. [PubMed: 30803032]

[21]. Kovalevich J, Santerre M, Langford D, Considerations for the Use of SH-SY5Y Neuroblastoma Cells in Neurobiology, Methods Mol Biol, 2311 (2021) 9–23. [PubMed: 34033074]

[22]. Acosta S, Lavarino C, Paris R, Garcia I, de Torres C, Rodríguez E, Beleta H, Mora J, Comprehensive characterization of neuroblastoma cell line subtypes reveals bilineage potential similar to neural crest stem cells, BMC Dev Biol, 9 (2009) 12. [PubMed: 19216736]

[23]. Twarog NR, Stewart E, Hammill CV, A AS, BRAID: A Unifying Paradigm for the Analysis of Combined Drug Action, Sci Rep, 6 (2016) 25523. [PubMed: 27160857]

[24]. Lane TR, Dyall J, Mercer L, Goodin C, Foil DH, Zhou H, Postnikova E, Liang JY, Holbrook MR, Madrid PB, Ekins S, Repurposing Pyramax® for the Treatment of Ebola Virus Disease: Additivity of the Lysosomotropic Pyronaridine and Non-Lysosomotropic Artesunate Antiviral Research, 182 (2020) 104908.

[25]. Sasaki T, Okuda K, Zheng W, Butrynski J, Capelletti M, Wang L, Gray NS, Wilner K, Christensen JG, Demetri G, Shapiro GI, Rodig SJ, Eck MJ, Jänne PA, The neuroblastoma-associated F1174L ALK mutation causes resistance to an ALK kinase inhibitor in ALK-translocated cancers, Cancer Res, 70 (2010) 10038–10043. [PubMed: 21030459]

[26]. Friboulet L, Li N, Katayama R, Lee CC, Gainor JF, Crystal AS, Michellys PY, Awad MM, Yanagitani N, Kim S, Pferdekamper AC, Li J, Kasibhatla S, Sun F, Sun X, Hua S, McNamara P, Mahmood S, Lockerman EL, Fujita N, Nishio M, Harris JL, Shaw AT, Engelman JA, The ALK inhibitor ceritinib overcomes crizotinib resistance in non-small cell lung cancer, Cancer Discov, 4 (2014) 662–673. [PubMed: 24675041]

[27]. Mossé YP, Lim MS, Voss SD, Wilner K, Ruffner K, Laliberte J, Rolland D, Balis FM, Maris JM, Weigel BJ, Ingle AM, Ahern C, Adamson PC, Blaney SM, Safety and activity of crizotinib for paediatric patients with refractory solid tumours or anaplastic large-cell lymphoma: a Children's Oncology Group phase 1 consortium study, Lancet Oncol, 14 (2013) 472–480. [PubMed: 23598171]

[28]. Wang HQ, Halilovic E, Li X, Liang J, Cao Y, Rakiec DP, Ruddy DA, Jeay S, Wuerthner JU, Timple N, Kasibhatla S, Li N, Williams JA, Sellers WR, Huang A, Li F, Combined ALK and MDM2 inhibition increases antitumor activity and overcomes resistance in human ALK mutant neuroblastoma cell lines and xenograft models, Elife, 6 (2017).

[29]. Suenaga Y, Kaneko Y, Matsumoto D, Hossain MS, Ozaki T, Nakagawara A, Positive auto-regulation of MYCN in human neuroblastoma, Biochem Biophys Res Commun, 390 (2009) 21–26. [PubMed: 19766596]

[30]. Ota Y, Yoda H, Inoue T, Watanabe T, Shinozaki Y, Takatori A, Nagase H, Targeting anaplastic lymphoma kinase (ALK) gene alterations in neuroblastoma by using alkylating pyrrole-imidazole polyamides, PLoS One, 16 (2021) e0257718. [PubMed: 34591871]

[31]. Goldschneider D, Horvilleur E, Plassa LF, Guillaud-Bataille M, Million K, Wittmer-Dupret E, Danglot G, de The H, Benard J, May E, Douc-Rasy S, Expression of C-terminal deleted p53 isoforms in neuroblastoma, Nucleic Acids Res, 34 (2006) 5603–5612. [PubMed: 17028100]

[32]. Nakamura Y, Ozaki T, Niizuma H, Ohira M, Kamijo T, Nakagawara A, Functional characterization of a new p53 mutant generated by homozygous deletion in a neuroblastoma cell line, Biochem Biophys Res Commun, 354 (2007) 892–898. [PubMed: 17276397]

[33]. Chiba K, Discovery of fingolimod based on the chemical modification of a natural product from the fungus, Isaria sinclairii, J Antibiot (Tokyo), 73 (2020) 666–678. [PubMed: 32681100]

[34]. Li MH, Hla T, Ferrer F, FTY720 inhibits tumor growth and enhances the tumor-suppressive effect of topotecan in neuroblastoma by interfering with the sphingolipid signaling pathway, Pediatr Blood Cancer, 60 (2013) 1418–1423. [PubMed: 23704073]

[35]. Lifshitz V, Priceman SJ, Li W, Cherryholmes G, Lee H, Makovski-Silverstein A, Borriello L, DeClerck YA, Yu H, Sphingosine-1-Phosphate Receptor-1 Promotes Environment-Mediated and Acquired Chemoresistance, Mol Cancer Ther, 16 (2017) 2516–2527. [PubMed: 28716816]

[36]. Chen L, Ruan Y, Wang X, Min L, Shen Z, Sun Y, Qin X, BAY 11-7082, a nuclear factor-κB inhibitor, induces apoptosis and S phase arrest in gastric cancer cells, J Gastroenterol, 49 (2014) 864–874. [PubMed: 23846545]

[37]. Krishnan N, Bencze G, Cohen P, Tonks NK, The anti-inflammatory compound BAY-11-7082 is a potent inhibitor of protein tyrosine phosphatases, FEBS J, 280 (2013) 2830–2841. [PubMed: 23578302]

[38]. Lee J, Rhee MH, Kim E, Cho JY, BAY 11-7082 is a broad-spectrum inhibitor with anti-inflammatory activity against multiple targets, Mediators Inflamm, 2012 (2012) 416036. [PubMed: 22745523]

[39]. Singh N, Baby D, Rajguru JP, Patil PB, Thakkannavar SS, Pujari VB, Inflammation and cancer, Ann Afr Med, 18 (2019) 121–126. [PubMed: 31417011]

[40]. Rauert-Wunderlich H, Siegmund D, Maier E, Giner T, Bargou RC, Wajant H, Stühmer T, The IKK inhibitor Bay 11-7082 induces cell death independent from inhibition of activation of NFκB transcription factors, PLoS One, 8 (2013) e59292. [PubMed: 23527154]

[41]. Zhang Q, Mao Z, Sun J, NF-κB inhibitor, BAY11-7082, suppresses M2 tumor-associated macrophage induced EMT potential via miR-30a/NF-κB/Snail signaling in bladder cancer cells, Gene, 710 (2019) 91–97. [PubMed: 31002892]

[42]. Zhang L, Xie J, Gan R, Wu Z, Luo H, Chen X, Lu Y, Wu L, Zheng D, Synergistic inhibition of lung cancer cells by EGCG and NF-κB inhibitor BAY11-7082, J Cancer, 10 (2019) 6543–6556. [PubMed: 31777584]

[43]. Viola K, Kopf S, Huttary N, Vonach C, Kretschy N, Teichmann M, Giessrigl B, Raab I, Stary S, Krieger S, Keller T, Bauer S, Hantusch B, Szekeres T, de Martin R, Jäger W, Mikulits W, Dolznig H, Krupitza G, Grusch M, Bay11-7082 inhibits the disintegration of the lymphendothelial barrier triggered by MCF-7 breast cancer spheroids; the role of ICAM-1 and adhesion, Br J Cancer, 108 (2013) 564–569. [PubMed: 23093227]

[44]. Yan Y, Qian H, Cao Y, Zhu T, Nuclear factor-κB inhibitor Bay11-7082 inhibits gastric cancer cell proliferation by inhibiting Gli1 expression, Oncol Lett, 21 (2021) 301. [PubMed: 33732377]

[45]. Chen W, Mook RA Jr., Premont RT, Wang J, Niclosamide: Beyond an antihelminthic drug, Cell Signal, 41 (2018) 89–96. [PubMed: 28389414]

[46]. Xu J, Shi PY, Li H, Zhou J, Broad Spectrum Antiviral Agent Niclosamide and Its Therapeutic Potential, ACS Infect Dis, 6 (2020) 909–915. [PubMed: 32125140]

[47]. Huang CT, Hsieh CH, Lee WC, Liu YL, Yang TS, Hsu WM, Oyang YJ, Huang HC, Juan HF, Therapeutic Targeting of Non-oncogene Dependencies in High-risk Neuroblastoma, Clin Cancer Res, 25 (2019) 4063–4078. [PubMed: 30952635]

[48]. Puhl AC, Fritch EJ, Lane TR, Tse LV, Yount BL, Sacramento CQ, Fintelman-Rodrigues N, Tavella TA, Maranhão Costa FT, Weston S, Logue J, Frieman M, Premkumar L, Pearce KH, Hurst BL, Andrade CH, Levi JA, Johnson NJ, Kisthardt SC, Scholle F, Souza TML, Moorman NJ, Baric RS, Madrid PB, Ekins S, Repurposing the Ebola and Marburg Virus Inhibitors Tilorone, Quinacrine, and Pyronaridine: In Vitro Activity against SARS-CoV-2 and Potential Mechanisms, ACS Omega, 6 (2021) 7454–7468. [PubMed: 33778258]

[49]. Lane TR, Massey C, Comer JE, Anantpadma M, Freundlich JS, Davey RA, Madrid PB, Ekins S, Repurposing the antimalarial pyronaridine tetraphosphate to protect against Ebola virus infection, PLoS Negl Trop Dis, 13 (2019) e0007890. [PubMed: 31751347]

[50]. Lane TR, Massey C, Comer JE, Freiberg AN, Zhou H, Dyall J, Holbrook MR, Anantpadma M, Davey RA, Madrid PB, Ekins S, Pyronaridine tetraphosphate efficacy against Ebola virus infection in guinea pig, Antiviral Res, 181 (2020) 104863. [PubMed: 32682926]

[51]. Croft SL, Duparc S, Arbe-Barnes SJ, Craft JC, Shin CS, Fleckenstein L, Borghini-Fuhrer I, Rim HJ, Review of pyronaridine anti-malarial properties and product characteristics, Malar J, 11 (2012) 270. [PubMed: 22877082]

[52]. Puhl AC, Gomes GF, Damasceno S, Godoy AS, Noske GD, Nakamura AM, Gawriljuk VO, Fernandes RS, Monakhova N, Riabova O, Lane TR, Makarov V, Veras FP, Batah SS, Fabro AT, Oliva G, Cunha FQ, Alves-Filho JC, Cunha TM, Ekins S, Pyronaridine Protects against SARS-CoV-2 Infection in Mouse, ACS Infect Dis, 8 (2022) 1147–1160. [PubMed: 35609344]

[53]. Ekins S, Freundlich JS, Clark AM, Anantpadma M, Davey RA, Madrid P, Machine learning models identify molecules active against the Ebola virus in vitro, F1000Res, 4 (2015) 1091. [PubMed: 26834994]

[54]. Villanueva PJ, Martinez A, Baca ST, DeJesus RE, Larragoity M, Contreras L, Gutierrez DA, Varela-Ramirez A, Aguilera RJ, Pyronaridine exerts potent cytotoxicity on human breast and hematological cancer cells through induction of apoptosis, PLoS One, 13 (2018) e0206467. [PubMed: 30395606]

[55]. NCI, NCI-60 Human Tumor Cell Lines Screen, 2020.

[56]. Jayaraman SD, Ismail S, Nair NK, Navaratnam V, Determination of pyronaridine in blood plasma by high-performance liquid chromatography for application in clinical pharmacological studies, J Chromatogr B Biomed Sci Appl, 690 (1997) 253–257. [PubMed: 9106050]

[57]. Mijanovic O, Petushkova AI, Brankovic A, Turk B, Solovieva AB, Nikitkina AI, Bolevich S, Timashev PS, Parodi A, Zamyatnin AA, Cathepsin D-Managing the Delicate Balance, Pharmaceutics, 13 (2021).

[58]. Ivankovic D, Chau KY, Schapira AH, Gegg ME, Mitochondrial and lysosomal biogenesis are activated following PINK1/parkin-mediated mitophagy, J Neurochem, 136 (2016) 388–402. [PubMed: 26509433]

[59]. Geisslinger F, Müller M, Vollmar AM, Bartel K, Targeting Lysosomes in Cancer as Promising Strategy to Overcome Chemoresistance-A Mini Review, Front Oncol, 10 (2020) 1156. [PubMed: 32733810]

[60]. Aits S, Jäättelä M, Lysosomal cell death at a glance, J Cell Sci, 126 (2013) 1905–1912. [PubMed: 23720375]

[61]. Krytska K, Ryles HT, Sano R, Raman P, Infarinato NR, Hansel TD, Makena MR, Song MM, Reynolds CP, Mossé YP, Crizotinib Synergizes with Chemotherapy in Preclinical Models of Neuroblastoma, Clin Cancer Res, 22 (2016) 948–960. [PubMed: 26438783]

[62]. Zhang L, Wu B, Baruchel S, Oral Metronomic Topotecan Sensitizes Crizotinib Antitumor Activity in ALK, Transl Oncol, 10 (2017) 604–611. [PubMed: 28666189]

[63]. Hande KR, Etoposide: four decades of development of a topoisomerase II inhibitor, Eur J Cancer, 34 (1998) 1514–1521. [PubMed: 9893622]

[64]. Bailly C, Pyronaridine: An update of its pharmacological activities and mechanisms of action, Biopolymers, 112 (2021) e23398. [PubMed: 33280083]

[65]. Anderson E, Havener TM, Zorn KM, Foil DH, Lane TR, Capuzzi SJ, Morris D, Hickey AJ, Drewry DH, Ekins S, Synergistic drug combinations and machine learning for drug repurposing in chordoma, Sci Rep, 10 (2020) 12982. [PubMed: 32737414]

[66]. Puhl AC, Gomes GF, Damasceno S, Godoy AS, Noske GD, Nakamura AM, Gawriljuk VO, Fernandes RS, Monakhova N, Riabova O, Lane TR, Makarov V, Veras FP, Batah SS, Fabro AT, Oliva G, Cunha FQ, Alves-Filho JC, Cunha TM, Ekins S, Pyronaridine Protects Against SARS-CoV-2 in Mouse, bioRxiv, (2021) 2021.2009.2030.462449.

[67]. Gaulton A, Hersey A, Nowotka M, Bento AP, Chambers J, Mendez D, Mutowo P, Atkinson F, Bellis LJ, Cibrian-Uhalte E, Davies M, Dedman N, Karlsson A, Magarinos MP, Overington JP, Papadatos G, Smit I, Leach AR, The ChEMBL database in 2017, Nucleic Acids Res, 45 (2017) D945–D954. [PubMed: 27899562]

[68]. Lane TR, Foil DH, Minerali E, Urbina F, Zorn KM, Ekins S, Bioactivity Comparison across Multiple Machine Learning Algorithms Using over 5000 Datasets for Drug Discovery, Mol Pharm, 18 (2021) 403–415. [PubMed: 33325717]

[69]. Russo DP, Zorn KM, Clark AM, Zhu H, Ekins S, Comparing Multiple Machine Learning Algorithms and Metrics for Estrogen Receptor Binding Prediction, Mol Pharm, 15 (2018) 4361–4370. [PubMed: 30114914]
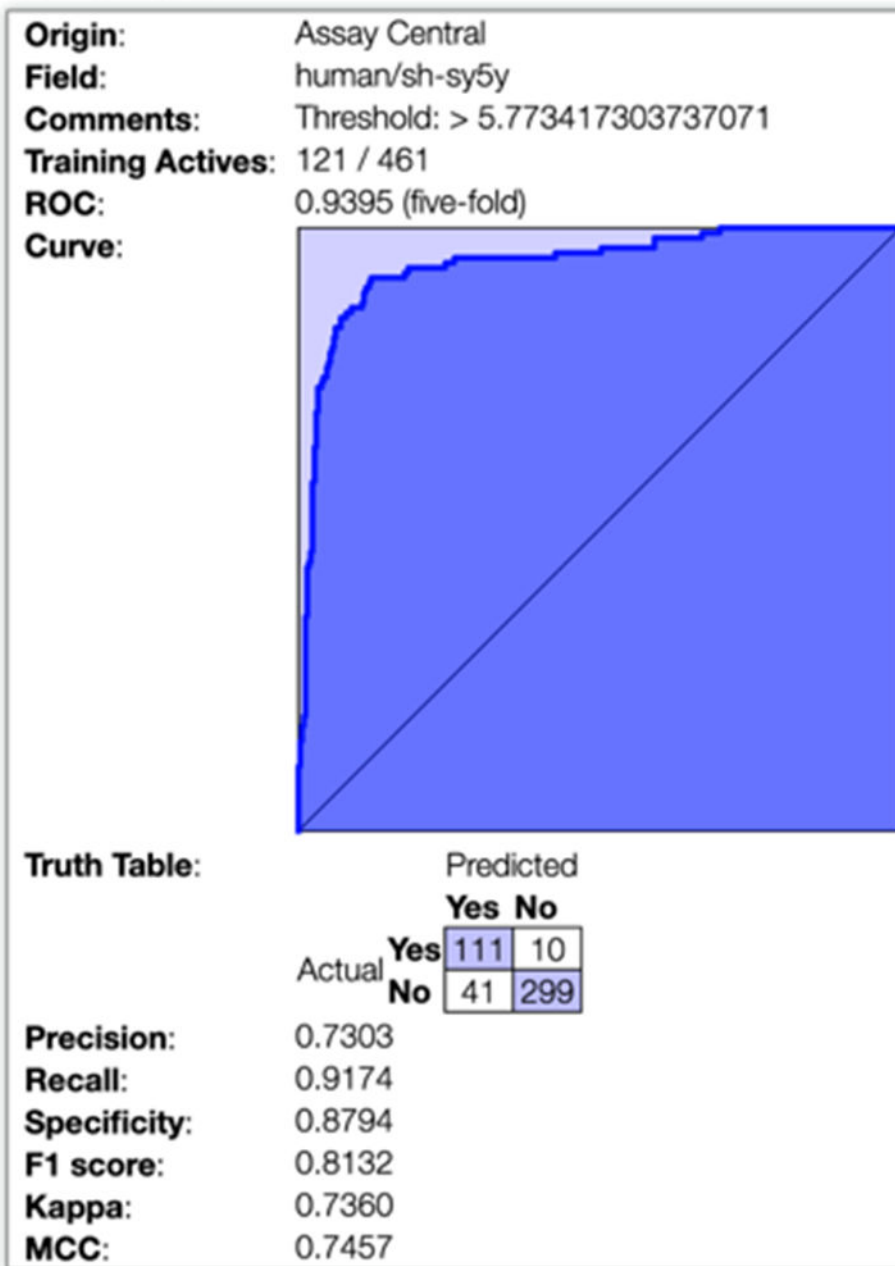
SH-SY5Y

Origin:	Assay Central
Field:	human/sh-sy5y
Comments:	Threshold: > 5.773417303737071
Training Actives:	121 / 461
ROC:	0.9395 (five-fold)
Curve:	

Truth Table:

		Predicted	
		Yes	**No**
Actual	**Yes**	111	10
	No	41	299

Precision:	0.7303
Recall:	0.9174
Specificity:	0.8794
F1 score:	0.8132
Kappa:	0.7360
MCC:	0.7457

Figure 1.
Five-fold ROC plot for the Bayesian neuroblastoma activity model. Abbreviations: Kappa = Cohen's Kappa, MCC = Matthews Correlation Coefficient.
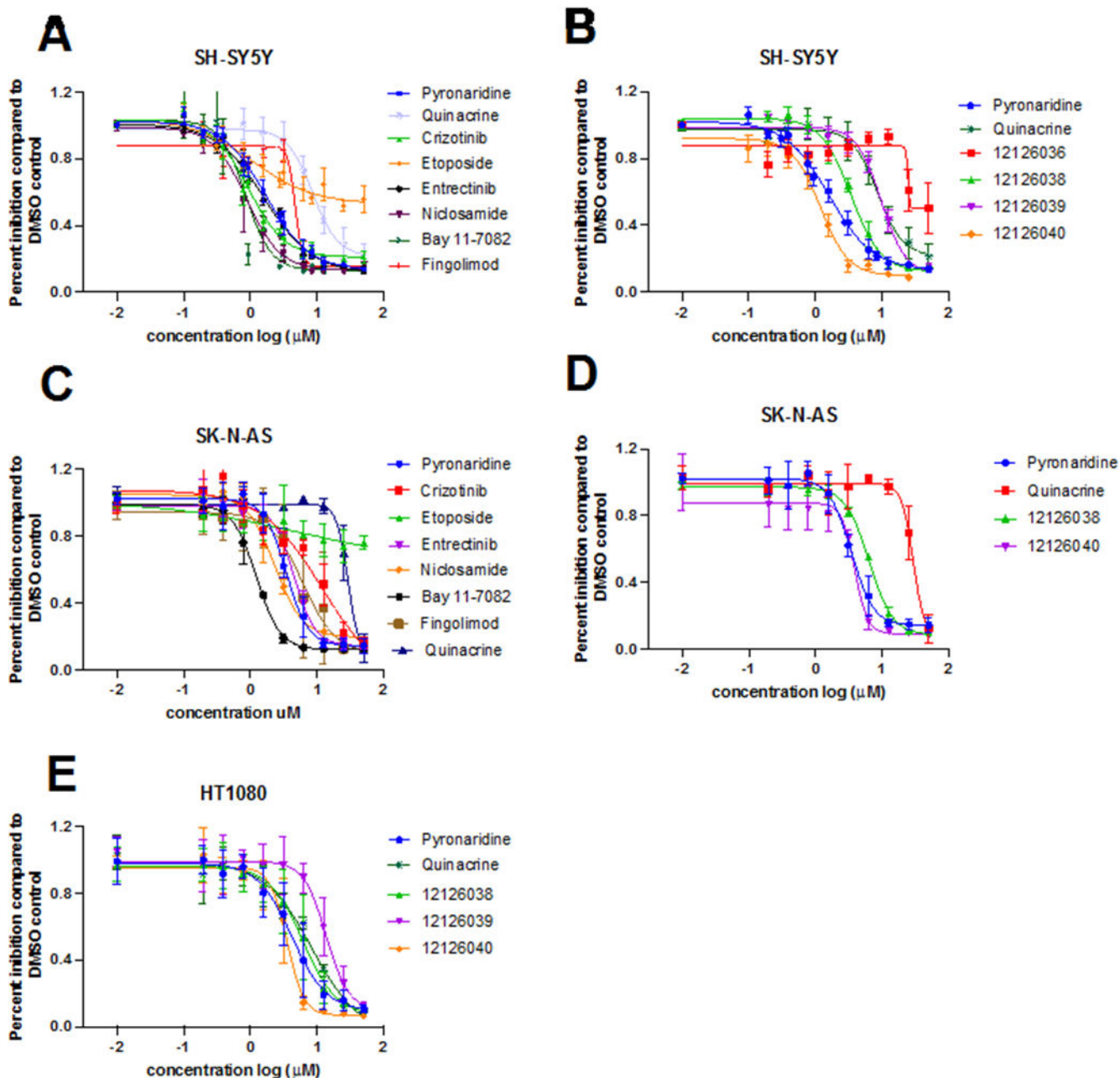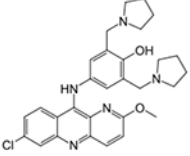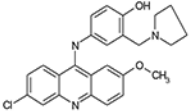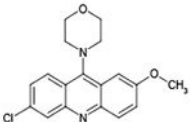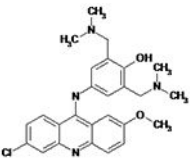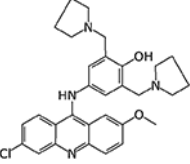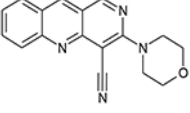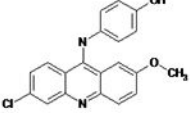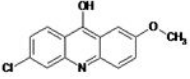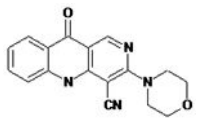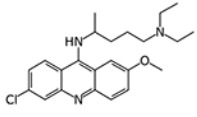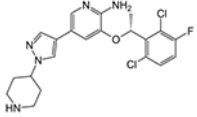
Figure 2.
Dose-response curves of compounds tested in SH-SY5Y (A, B), SK-N-AS (C, D) and HT-1080 (E). Control compounds crizotinib IC_{50} 0.92 μM in SH-SY5Y and IC_{50} 12.12 μM in SK-N-AS and entrectinib IC_{50} 1.60 in SH-SY5Y and IC_{50} 4.47 μM in SK-N-AS.

Table 1.

Compounds tested in NB SH-SY5Y and SK-N-AS, and fibrosarcoma HT-1080. Blank: not tested NA: Ambiguous fit.

Structure	Compound	Average IC$_{50}$ SH-SY5Y	Average IC$_{50}$ SK-N-AS	Average IC$_{50}$ HT-1080
	Pyronaridine	1.70 μM	3.45 μM	4.23 μM
	12126040	1.20 μM	3.86 μM	3.6 μM
	12126036	NA	NA	NA
	12126038	3.41 μM	5.40 μM	6.09 μM
	12126039	9.70 μM	NA	13.77 μM
	12126035	Drug did not inhibit at 5 μM	NA	NA
	12126037	Drug did not inhibit at 5 μM	NA	NA
	12126072	Drug did not inhibit at 5 μM	NA	NA

Structure	Compound	Average IC$_{50}$ SH-SY5Y	Average IC$_{50}$ SK-N-AS	Average IC$_{50}$ HT-1080
	10326099	Drug did not inhibit at 5 μM	NA	NA
	Quinacrine	8.57 μM	NA	29.1 μM
	Crizotinib	0.92 μM	12.12 μM	NA

Table 2:

Combination therapies and BRAID analysis.

The variable κ represents a quantitative synergy value where $\kappa < 0$ implies antagonism, $\kappa = 0$ implies additivity, and $\kappa > 0$ implies synergy. As an additional reference, "strong synergy" corresponds to $\kappa = 2.5$, "mild synergy" corresponds to $\kappa = 1$, "mild antagonism" corresponds to $\kappa = -0.66$, and "strong antagonism" corresponds to $\kappa = -1$.

Compound 1	Compound 2	K (average of 4 experiments)
Pyronaridine	Crizotinib	−0.640
Pyronaridine	Etoposide	−0.746
Crizotinib	Etoposide	3.46